

# Magma–sediment interaction during the emplacement of syn-sedimentary silicic and mafic intrusions and lavas into and onto Triassic strata (Circum-Rhodope Belt, northern Greece)

ARGYRO ASVESTA<sup>1</sup> and SARANTIS DIMITRIADIS<sup>2</sup>

<sup>1</sup>Department of Geotechnology and Environmental Engineering, Technological Educational Institute (TEI) of Western Macedonia, Kila, 50100 Kozani, Greece; asvesta@teiko.gr

<sup>2</sup>Department of Geology, Aristotle University of Thessaloniki, 54124 Thessaloniki, Greece; sarantis@geo.auth.gr

(Manuscript received April 5, 2012; accepted in revised form December 11, 2012)

**Abstract:** Within the Circum-Rhodope Belt in northern Greece, Middle Triassic neritic carbonate metasediments are locally intercalated with quartz-feldspar-phyric metarhyolites. In the same belt, Upper Triassic pelagic lime-marl-layered metasediments are similarly intercalated with low-grade metamorphosed basalt, dolerite and minor andesite and trachydacite. We interpret these sequences as due to magmatism active during the rifting event that eventually led to the opening of the Vardar Ocean. Despite the overprint of Late Jurassic deformation and low greenschist metamorphism, peperitic textures produced by magma–wet sediment interaction are well preserved at the contacts between the silicic volcanic rocks and the originally wet unconsolidated neritic carbonate sediments, suggesting contemporaneous magmatism and sedimentation. The mafic and intermediate volcanic rocks lack peperitic textures at their contacts with the pelagic sedimentary rocks. Thin margin parallel banding in the sedimentary members of the sequence indicates thermally affected original contacts with the mafic volcanic rocks only locally and at a microscopic scale. The absence of peperite in this case is attributed to the consolidated state of the sediments at the time of the mafic magma emplacement.

**Key words:** Triassic, Circum-Rhodope Belt, contact metamorphism, low greenschist metamorphism, carbonate sediments, basalt and dolerite, rhyolitic peperites.

## Introduction

When magma interacts with unconsolidated sediment, breccia is generated by disintegration of magma and mingling with the host sediment. This breccia facies is called peperite (White et al. 2000; Skilling et al. 2002). Peperite develops in a wide variety of successions but it is very commonly associated with intrusions and lavas in subaqueous (submarine) sedimentary sequences. Peperite occurs in any tectonic setting where magma or lava and unconsolidated sediment are able to interact, especially where volcanism is accompanied by continuous sedimentation in a subsiding basin. A wide variety of peperite compositional and textural types are known (Skilling et al. 2002).

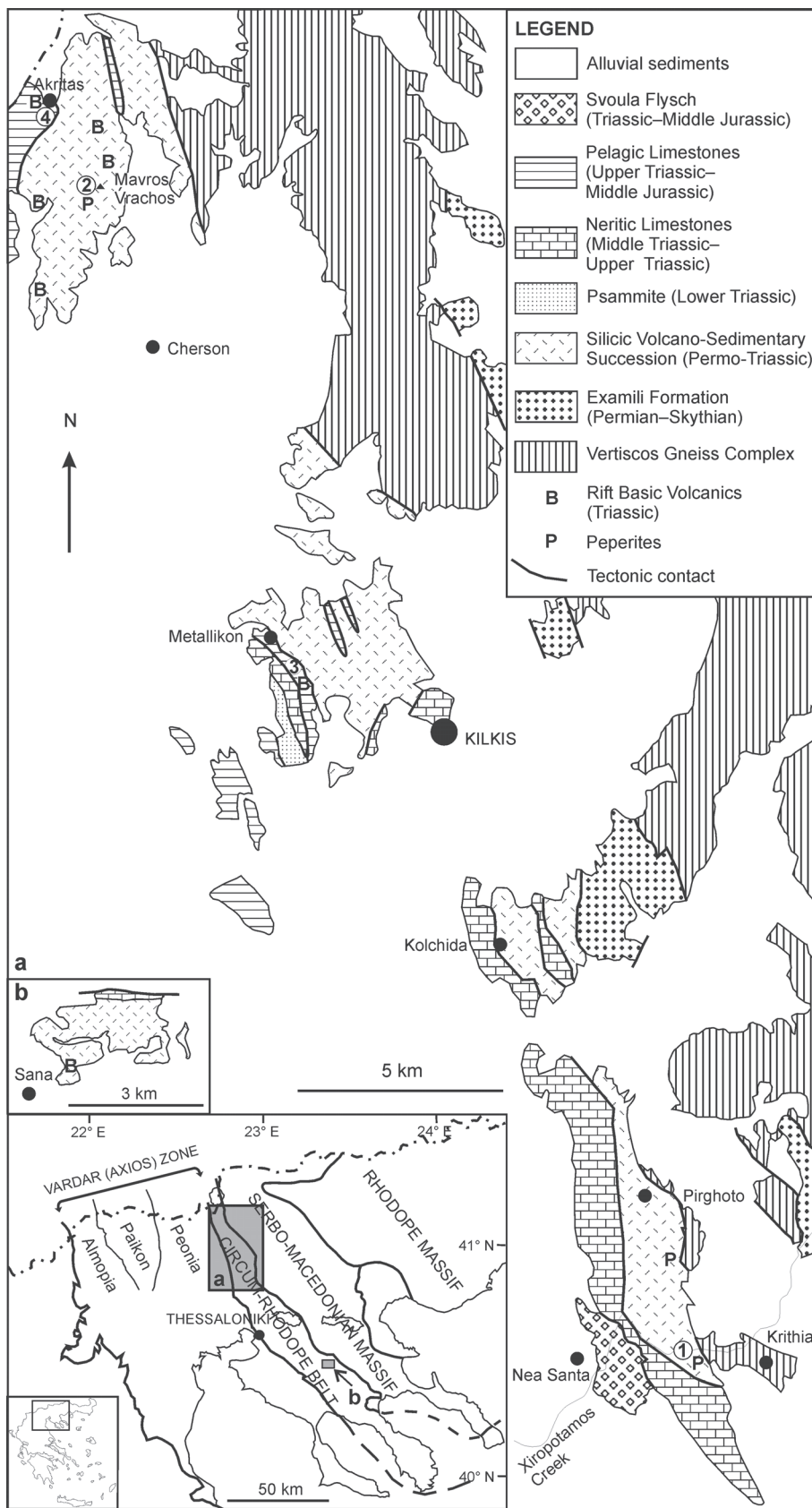
The recognition of peperite in a succession provides the evidence for the interaction of magma with unconsolidated, commonly wet, sediment and is an effective way of determining the synchronism of magmatism and sedimentation. Therefore, it contributes to the relative chronology and is a valuable tool in reconstructing facies architecture and paleoenvironments. Moreover, the presence of peperite at the roof of a concordant igneous body helps distinguish true lavas from intrusions (Skilling et al. 2002 and references therein).

In this paper, we study the products of magma–sediment interaction in a Permo-Triassic volcano-sedimentary complex at the eastern part of the Vardar (Axios) Zone, within the Circum-Rhodope Belt, northern Greece. Although the rocks are recrystallized under conditions of greenschist facies, their original fabrics are well preserved and much can

be inferred about their origin. Peperites were formed where a quartz-feldspar-phyric partly extrusive rhyolitic crypto-dome and rhyolitic sills intruded Triassic neritic carbonate sediments. Descriptions of the newly recognized peperite occurrences are provided. Specific criteria to discriminate peperite from other mixed volcanic-sediment breccia facies are discussed. Where mafic and intermediate rocks are in contact with Triassic pelagic sediments, peperite is absent; instead, small scale contact metamorphic phenomena are present. The cause of the absence of peperite in this case is discussed.

## Geological setting

In the easternmost part of the Vardar (Axios) Zone in Greece (the Peonias subzone of Mercier 1966/68), within the Circum-Rhodope Belt of Kockel et al. (1971, 1977), a Permo-Triassic volcano-sedimentary complex (~85 km long and 4–7 km wide) crops out discontinuously in NNW–SSE direction (Fig. 1). It bounds the western margin of the Vertiscos Complex, which contains orthogneisses of Early Paleozoic age (Kockel et al. 1971, 1977; Kauffmann et al. 1976; Kourou 1991; Sidiropoulos 1991; Asvesta 1992; Himmerkus et al. 2009; Asvesta & Dimitriadis 2010a). The Vertiscos Gneiss Complex is in contact with the Permo-Triassic volcano-sedimentary complex in a series of north-eastwards steeply dipping reverse faults which also run parallel to the NNW–SSE oriented belt of the Peonian Ophiolites (Mercier 1966/68; Asvesta & Dimitriadis 2010a). The Permo-Triassic volcano-



sedimentary complex is now overturned, telescoped and tectonically sandwiched between the south-westwards steeply thrust Vertiscos Gneisses and the Peonian Ophiolites, within which, as well as within the Vertiscos itself, westward or south-westward directed thrusts are also present. This tectonic picture is the end result of probably two similarly directed compression events, a first one of Late Jurassic and a second one of Early Tertiary age (Mercier 1966/68; Kockel et al. 1971, 1977).

**Local stratigraphy**

The Permo-Triassic volcano-sedimentary complex comprises sub-aerial to submarine volcanic and sedimentary rocks. From bottom to top (Fig. 2), it is composed of: a) The Examili Formation; b) The Silicic Volcano-Sedimentary (SVS) succession; c) The neritic and pelagic carbonate sedimentary facies of the Svoula Formation.

All the contacts between the above formations are now tectonic but it is generally accepted (Mercier 1966/68; Kauffmann et al. 1976; Kockel et al. 1977; Stais & Ferrière 1991; Asvesta 1992; Dimitriadis & Asvesta 1993; Ferrière & Stais 1995; Meinhold et al. 2009; Asvesta & Dimitriadis 2010a) that they represent secondarily tectonized original stratigraphic contacts. All the rocks are deformed with a northeast dipping cleavage and have been metamorphosed to low-greenschist facies during a Late Jurassic Alpine event. Despite this, primary sedimentary and volcanic features are well preserved and the prefix “meta-” is omitted in the following descriptions.

The Examili Formation consists of terrigenous, immature, poorly sorted, unfossiliferous, slightly metamorphosed arkosic sandstones and conglomerates. It is generally believed to be Permian-Skythian in age (Kauffmann 1976; Kauffmann et al. 1976; Kockel et al. 1977) because of the time constraints imposed by the stratigraphically over-

**Fig. 1.** Geological map of Permo-Triassic volcano-sedimentary complex in the Circum-Rhodope Belt illustrates the main lithostratigraphic units. Studied locations (1, 2, 3, 4) are noted. Modified after Mercier (1966/68), Kockel & Ioannides (1979) and Asvesta (1992).

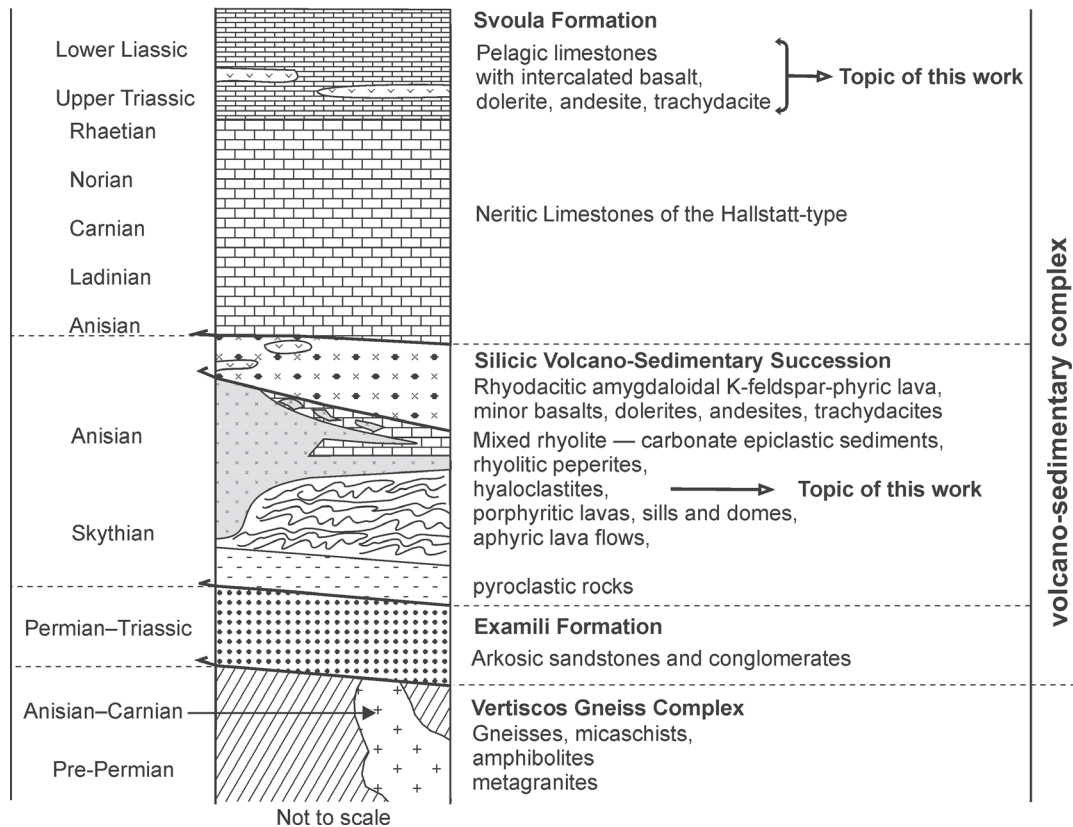


**Fig. 2.** Synthetic columnar tectonostratigraphic succession of Permo-Triassic volcano-sedimentary complex in the Circum-Rhodope Belt of northern Greece. Modified after Mercier (1966/68), Kockel & Ioannides (1979), Asvesta (1992), Meinhold et al. (2009) and Asvesta & Dimitriadis (2010a).

lying Silicic Volcano-Sedimentary (SVS) succession. The volcanic rocks of the SVS succession are probably Early to Middle Triassic in age, based on the finding of micro- and macro-fauna in the overlying and interbedded limestones (e.g. Dimitriadis & Asvesta 1993; Ferrière & Stais 1995) and on U-Pb dating of rhyolitic zircons, which has yielded an age of 240 Ma (R. Frei, unpublished report; in Kostopoulos et al. 2001). Furthermore, Meinhold et al. (2009) based on U-Pb (in zircon) geochronology propose a Permian-Triassic age for the sedimentary rocks of the Examili Formation, in accordance with previous studies.

The Silicic Volcano-Sedimentary (SVS) succession (Asvesta & Dimitriadis 2010a) or “Volcanosedimentary series” (Mercier 1966/68; Kockel et al. 1977) or “Pirghoto Formation” (Ferrière & Stais 1995; Meinhold et al. 2009) can be divided into two parts (Asvesta & Dimitriadis 2010a). The lower part comprises rhyolitic pyroclastic rocks (lapilli and minor accretionary lapilli tuffs) and aphyric and porphyritic lavas, most likely emplaced in a subaerial-coastal environment. The upper part comprises rhyolitic quartz-feldspar-phyric lavas, domes, hyaloclastites, sills interbedded with neritic carbonate sedimentary rocks composed of rhyolitic and carbonate fragments, all suggesting emplacement in a submarine environment. Peperites were found near Nea Santa (Loc. 1 in Fig. 1) and Akritas (Loc. 2 in Fig. 1) villages. They reveal original contacts between rhyolitic porphyries and carbonate sedimentary facies

of the overlying Triassic neritic limestone of Svoula Formation (Asvesta 1992; Dimitriadis & Asvesta 1993; Asvesta & Dimitriadis 2010a,b) and are a topic of this work.

Rhyolitic porphyry dykes intruding the Vertiscos Gneisses near Nea Santa (Asvesta 1992; Asvesta & Dimitriadis 2010a) and Zagliveri (Kauffmann et al. 1976) villages, not far from the exposed SVS succession, are probably feeder dykes to the volcanic rocks.

The part of the SVS succession that is exposed in the area between Akritas village and the city of Kilikis comprises in addition rhyodacitic amygdaloidal K-feldspar-phyric lavas (named as “Doiranite” by Osswald 1938). In the area between Akritas village and Cherson village (Fig. 1), these silicic lavas are locally intercalated (intruded or interstratified) with subordinate basalt, dolerite, andesite and trachydacite, named herein as “Triassic Rift Basic Volcanics” (Asvesta 1992; Dimitriadis & Asvesta 1993). Small exposures of these lavas also occur further south, near Sana village (Fig. 1). A banded iron formation (Mavros Vrachos Hill) near Akritas village (Fig. 1) is genetically associated with this volcanism (Tsamadouridis & Choriantopoulou 1990; Asvesta 1992).

The neritic carbonate sedimentary facies of the Svoula Formation (Kauffmann et al. 1976; Kockel et al. 1977) contains conodonts, brachiopods, echinoderms, foraminifera, corals and crinoids of Middle and Late Triassic age (Mercier 1966/68; Kauffmann et al. 1976; Stais & Ferrière 1991; Ferrière & Stais 1995). It is composed of:

- a) Dark grey bedded limestone carrying lenses of reddish to pink flaser limestone rich in conodonts (age Carnian);  
 b) White, massive or thick-bedded, recrystallized limestone (age Ladinian);  
 c) Yellow to whitish, thick-bedded dolomite, alternating with limestone;  
 d) Black, ferruginous, thin-bedded limestone with brachiopods (age Anisian);  
 e) Dark grey, thin-bedded, detrital limestone alternating with whitish sandstone layers and fine-grained conglomerate.

The neritic limestone facies pass upwards into the pelagic sedimentary facies of the Metallikon and Megali Sterna Units. The pelagic sedimentary facies of the Metallikon Unit is composed of dark grey, in places red, thin-bedded, micritic and biosparitic limestones with intercalations of yellow marls, dark grey shales and calc-schists. In the area near Metallikon village (Loc. 3 in Fig. 1) it contains interstratifications of altered dolerite and basalt of the Triassic Rift Basic Volcanics (Stais & Ferrière 1991; Asvesta 1992; Dimitriadis & Asvesta 1993; Ferrière & Stais 1995). According to Ferrière & Stais (1995) these mafic rocks are probably of Late Ladinian-Late Triassic age, as is indicated by the occurrence of the foraminifera "*Aulotortus* ex. gr. *communis*" (Kristan) and "*Agathammina austroalpina*" (Kristan-Tollmann & Tollmann) in intercalated sedimentary units and the presence of Carnian conodonts in the overlying limestone. Mercier (1966/68) and Kauffmann et al. (1976) had attributed an Early Jurassic age to these rocks.

The pelagic facies of the Megali Sterna Unit is of Late Norian age (Kauffmann et al. 1976) and is composed of grey, bluish and white thin-bedded recrystallized pelagic platy limestones, with lenses of white-grey thick-bedded limestones and layers of shales and calc-schists. In the lower part of the series, which is intensely folded, alternations of phyllites and platy limestones occur (Mercier 1966/68; Kauffmann et al. 1976). In the area to the south of Akritas village (Loc. 4 in Fig. 1) intercalations of basalt and dolerite and minor andesite and trachydacite of the Triassic Rift Basic Volcanics (now-metamorphosed to greenschist facies) have been found in among the pelagic lime-marl-layered sedimentary facies of Megali Sterna Unit (Asvesta 1992; Dimitriadis & Asvesta 1993). The interaction between mafic units and pelagic sedimentary units is a topic of this work.

### Syn-sedimentary intrusions and lavas

Representative chemical analyses of the silicic porphyries associated with peperites and the mafic and intermediate volcanic rocks are given in Table 1. The immobile element ratios provide reliable information on primary geochemistry and petrogenetic affinity. On the basis of classification diagrams (Winchester & Floyd 1977), the silicic porphyries of Nea Santa and Akritas areas are characterized as rhyolites and rhyodacites, the mafic volcanic rocks of Akritas-Metallikon as sub-alkaline basalts, and the intermediate volcanic rocks of Akritas as andesites and trachydacites (Fig. 3). All magma types have Nb/Y ratios less than 0.67 indicating their sub-alkaline affinity. The silicic volcanic rocks show a within plate granite (WPG) to volcanic arc granite (VAG) chemical

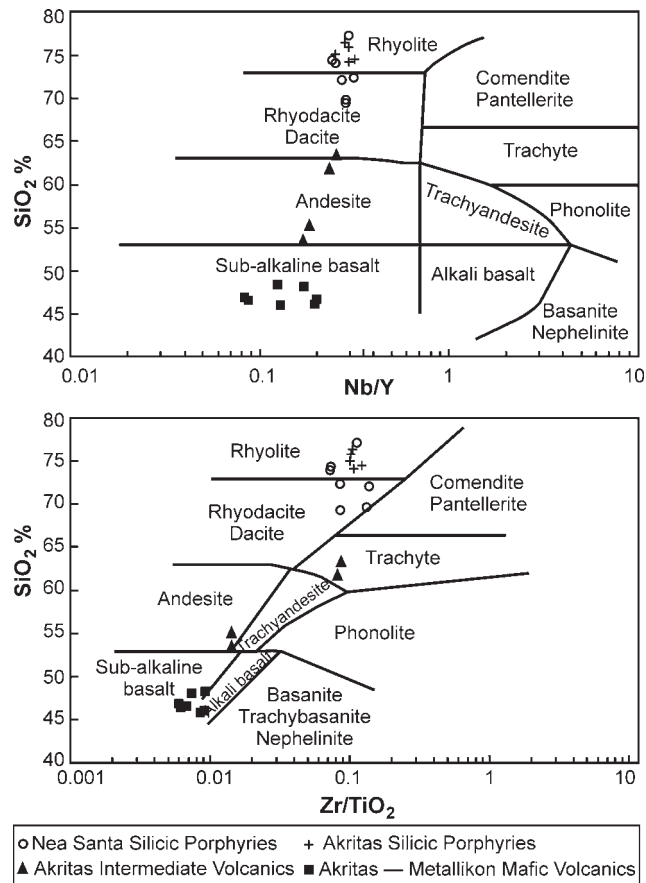


Fig. 3. On the SiO<sub>2</sub> vs. Nb/Y and SiO<sub>2</sub> vs. Zr/TiO<sub>2</sub> classification diagrams (after Winchester & Floyd 1977), silicic porphyries associated with peperites are classified as rhyolites-rhyodacites, mafic volcanic rocks as sub-alkaline basalts and intermediated volcanic rocks as andesites and trachytes or dacites.

character and represent a calc-alkaline silicic suite (Asvesta 1992; Asvesta & Dimitriadis 2010a). The mafic volcanic rocks show mid-ocean ridge basalt (MORB) to within plate basalt (WPB) affinity and are interpreted as volcanic rocks of a Triassic rift-related tholeiitic suite ("Triassic Rift Basic Volcanics"; Asvesta 1992; Dimitriadis & Asvesta 1993).

### Silicic rocks

Silicic syn-sedimentary volcanic rocks are porphyritic and contain quartz and K-feldspar phenocrysts (1 to 4 mm in size) and fewer small-sized albite crystals. Phenocrysts amount to about 30 % of the rock. Accessory minerals are zircon, oxidized biotite and disseminated microgranules of magnetite. Subhedral quartz phenocrysts show round edges and embayments filled with the groundmass. They display undulose extinction; some crystals, however, have been annealed and recrystallized to granoblastic aggregates. K-feldspar phenocrysts are kaolinized and sericitized, partly corroded, euhedral to subhedral perthitic microcline (exsardine) and some of them are twinned. The groundmass is mostly composed of quartz and sericite, as a result of low-grade metamorphism. A curved, stringy sericite mesh

**Table 1:** Representative chemical analyses of Triassic syn-sedimentary volcanic rocks.

Location Rock Sample	Nea Santa silicic							Akritas silicic				
	A49	A66	A626	A629	A630	A631	A637	A678	A5	A757	A670	A671
SiO <sub>2</sub> (wt. %)	74.41	74.15	69.45	69.79	77.33	72.20	72.37	76.52	75.09	74.53	75.89	74.26
Al <sub>2</sub> O <sub>3</sub>	12.20	12.96	5.96	15.98	11.27	13.46	13.58	11.83	12.08	12.71	12.07	12.65
Fe <sub>2</sub> O <sub>3</sub>	1.41	1.05	2.08	2.11	1.25	1.55	1.53	0.67	1.81	1.97	2.07	2.05
MgO	0.11	0.41	0.79	0.75	0.06	0.00	n.d.	0.23	0.42	0.55	0.15	0.19
CaO	0.20	0.12	0.16	0.15	0.31	0.01	0.01	0.14	0.05	0.06	0.01	0.01
Na <sub>2</sub> O	1.00	0.56	2.18	2.01	1.52	0.14	0.13	n.d.	0.18	2.02	n.d.	0.00
K <sub>2</sub> O	9.20	9.10	7.55	7.59	7.44	11.76	11.77	9.40	8.57	7.12	9.00	10.10
TiO <sub>2</sub>	0.18	0.17	0.22	0.22	0.13	0.12	0.12	0.25	0.18	0.36	0.18	0.19
MnO	0.00	0.01	n.d.	0.00	0.01	0.01	0.01	n.d.	0.02	0.00	0.01	0.00
P <sub>2</sub> O <sub>5</sub>	0.05	0.06	0.04	0.04	0.02	0.02	0.02	0.13	0.02	0.05	0.04	0.03
Total	98.76	98.59	98.43	98.64	99.34	99.27	99.54	99.17	98.42	99.37	99.42	99.48
Ni (ppm)	4	5	11	6	6	8	8	9	4	11	21	8
Cr	1	1	n.d.	2	2	3	1	6		7	0	2
V	7	8	1	4	1	0	5	6	5	10	4	4
Sc	1	3	1	4	1	2	n.d.	5	4	4	4	5
Cu	4	3	28	n.d.	1	11	n.d.	9	17	n.d.	n.d.	n.d.
Zn	14	42	12	46	25	41	19	34	39	47	20	19
Sr	12	14	32	33	12	12	9	23	10	17	14	7
Rb	305	312	20	297	240	270	310	204	240	152	235	258
Ba	455	367	24	230	152	156	726	1381	734	618	632	575
Pb	18	13	32	3	25	25	5	1	8	n.d.	2	3
Th	23	25	21	28	19	19	13	10	25	18	19	18
Zr	132	124	187	287	149	166	102	263	180	435	184	202
Nb	9	10	18	20	16	16	10	13	13	16	13	13
Y	37	40	63	70	54	59	32	46	52	50	44	44
La	33	35	37	61	33	32	23	29	36	12	43	45
Ce	62	68	92	116	62	66	55	55	81	29	97	103
Nd	29	31	41	48	29	29	27	40	42	18	42	45

Location Rock Sample	Metallikon mafic KM	Akritas mafic						Akritas intermediate			
		A681	B39	B43	B80	B127	B128	B46	B116	B121	B122
SiO <sub>2</sub> (wt. %)	48.38	46.55	46.70	48.19	46.95	46.00	46.17	55.16	53.57	61.90	63.47
Al <sub>2</sub> O <sub>3</sub>	14.91	16.40	15.89	15.16	17.27	15.78	16.03	13.20	13.18	14.21	13.67
Fe <sub>2</sub> O <sub>3</sub>	10.14	9.02	11.31	10.22	8.82	11.09	12.24	13.50	13.30	8.94	9.73
MgO	7.57	8.95	8.54	6.89	10.75	9.08	8.03	4.20	3.92	1.65	0.87
CaO	6.08	10.10	9.23	10.26	6.53	10.74	8.49	2.13	3.32	2.15	1.69
Na <sub>2</sub> O	4.78	1.44	2.20	3.52	1.45	1.91	3.19	3.81	4.01	6.96	5.77
K <sub>2</sub> O	0.06	2.20	1.37	0.34	3.09	0.80	0.29	3.28	1.93	0.39	1.37
TiO <sub>2</sub>	1.49	1.24	1.94	1.72	1.20	1.72	2.22	2.50	2.50	0.96	0.84
MnO	0.14	0.18	0.17	0.19	0.17	0.18	0.20	0.19	0.23	0.17	0.18
P <sub>2</sub> O <sub>5</sub>	0.13	0.11	0.19	0.17	0.10	0.16	0.25	0.39	0.40	0.23	0.20
Total	93.68	96.19	97.54	96.66	96.33	97.46	97.11	98.36	96.36	97.56	97.79
Ni (ppm)	61	143	122	54	152	142	92	8	7	6	7
Cr	145	317	319	430	381	359	254	2	0	1	1
V	242	204	259	280	197	257	281	154	135	3	2
Sc	38	33	39	55	34	38	40	30	32	23	20
Cu	42	38	25	101	52	94	44	n.d.	n.d.	n.d.	n.d.
Zn	71	86	84	84	71	103	111	156	156	132	163
Sr	270	580	313	631	100	1156	1047	71	98	120	194
Rb	1	68	38	9	133	33	12	110	51	18	51
Ba	2	269	131	52	337	124	56	161	207	99	183
Pb	1	n.d.	3	4	2	2	n.d.	1	2	3	6
Th	2	n.d.	n.d.	n.d.	n.d.	n.d.	n.d.	6	5	16	15
Zr	137	77	132	127	72	146	201	359	354	784	732
Nb	4	2	6	5	2	4	7	15	12	26	25
Y	32	23	30	29	24	31	36	82	71	111	99
La	16	n.d.	0	1	5	1	5	26	26	37	44
Ce	22	9	16	12	6	8	17	64	69	104	101
Nd	9	8	12	10	9	7	12	38	41	66	57

Whole-rock analyses were performed with a Phillips PW1450/20 X-ray fluorescence spectrometer (XRF) at the Department of Geology and Geophysics of the University of Edinburgh using standard procedures. Major elements were analysed on fused glass discs and trace elements on pressed powder pellets. **n.d.**— not detected.

present in some places mimics perlite cracking, suggesting an originally glassy character of the groundmass.

#### *Mafic and intermediate rocks*

Mafic volcanic rocks, exposed near Akritas and Metallikon villages, are altered doleritic dykes and basaltic lavas (Fig. 4A). In many places, they preserve relict ophitic texture

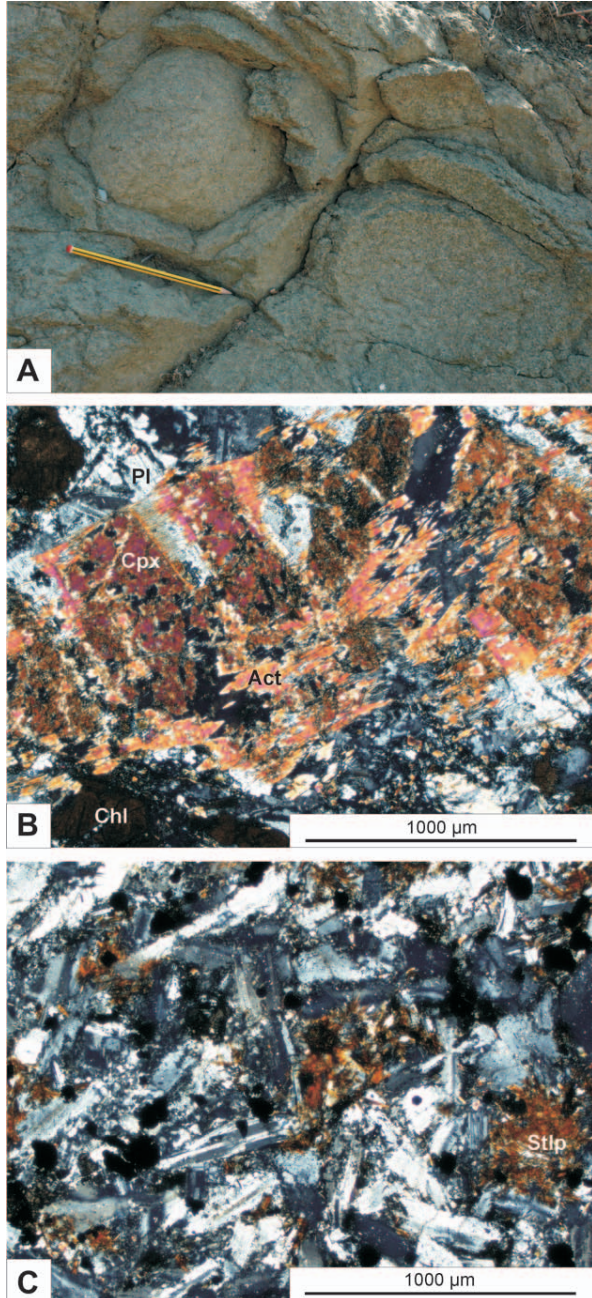


**Fig. 4.** A — Spheroidal weathering in mafic volcanic rock exposed near Metallikon village. B — Relict clinopyroxene (Cpx) and plagioclase (Pl) crystals (ophitic texture). Actinolite (Act) and chlorite (Chl) are products of greenschist metamorphism (crossed polars). C — Intermediate volcanic rock showing hyalo-ophitic texture with plagioclase crystals and stilpnomelane (Stlp) (recrystallized ferrous glass). Note high concentration of magnetite grains (crossed polars).

and have disequilibrium mineral assemblages, characterized by relict subhedral plagioclase crystals, enclosed in relict clinopyroxene crystals. The clinopyroxene is diopside, largely converted to actinolite and chlorite (Fig. 4B), as a result of greenschist facies metamorphism. Microprobe analyses of pyroxene and amphibole are present in Table 2. Albite, zoisite, clinozoisite and calcite have been formed after the primary plagioclase. Sphene and leucoxene ( $\text{TiO}_2 \cdot n\text{H}_2\text{O}$ ) have replaced ilmenite; relics of the last are seen in the centre of leucoxene assemblages. Quartz, pyrite and magnetite crystals are also present.

Intermediate volcanic rocks are exposed only near Akritas village. They have relict hyalo-ophitic texture. Plagioclase crystals occur in a mass of stilpnomelane that has probably been formed by crystallization of ferrous glassy groundmass (Fig. 4C). In the andesites, metamorphic biotite has grown parallel to schistosity and tiny magnetite crystals are concentrated in laminae.

#### **Field evidence for magma–sediment interaction**

A variety of magma–wet sediment interaction features are well preserved at many locations of the studied area (Fig. 1). Peperitic textures of the Nea Santa and Akritas rhyolites reveal interaction between silicic magma and wet unconsolidated neritic carbonate sediment. Thermal contact phenomena in pelagic sedimentary rocks suggest interaction between mafic magma and pelagic lime-marl-layered sediment.

#### *Peperitic textures and hyaloclastite associated with the Nea Santa rhyolite*

The Nea Santa rhyolitic porphyry is mostly represented by a partly extrusive dome (~1 km in diameter) (Loc. 1 in Fig. 1) that had intruded into wet unconsolidated carbonate sediments (Asvesta & Dimitriadis 2010a,b). The dome is coherent and non-vesicular in its core but its external upper marginal sector is perlitic and contains lithophysae in-filled with quartz. In places, the contact between the rhyolitic porphyry and the carbonate sedimentary rock is gradational, forming a mixed breccia facies. This breccia is composed of rhyolite clasts in a carbonate matrix and is interpreted as peperite (Asvesta & Dimitriadis 2010a).

On the basis of the dominant shape of the juvenile clasts, two different textural types of peperite are recognized at the Nea Santa rhyolite dome: (1) the fluidal and (2) the blocky, according to the nomenclature of Busby-Spera & White (1987). Both the fluidal and the blocky peperites have been subjected to mineralogical and textural modifications probably due to hydrothermal alteration (coeval to or following the peperite genesis) and later low-grade regional metamorphism. Apart from the dome itself, syn-sedimentary rhyolitic porphyry stubby sills or hyaloclastic lavas are intercalated with the neritic carbonate sedimentary rocks and present micro-peperitic textures at their margins. Resedimented hyaloclastite breccia facies and polymictic rhyolite-carbonate epiclastic sedimentary facies in the vicinity testify to the partly extrusive nature of the rhyolitic dome (Asvesta & Dimitriadis 2010a,b).

**Table 2:** Representative electron microprobe analyses of pyroxene and amphibole from mafic volcanic rocks and garnet (product of contact metamorphism) from the lime-marl-layered sedimentary rocks (Akritas area).

Mineral	Pyroxene	Amphibole	Garnet
Sample no.	B58	B58	B59
Location	(4) in Fig. 1	(4) in Fig. 1	(4) in Fig. 1
SiO <sub>2</sub> (wt. %)	52.69	53.26	38.74
TiO <sub>2</sub>	0.00	0.01	0.11
Al <sub>2</sub> O <sub>3</sub>	0.40	1.68	16.76
Cr <sub>2</sub> O <sub>3</sub>	0.09	–	0.00
*FeO	9.34	13.70	6.82
MnO	0.39	0.28	0.13
MgO	11.95	14.24	0.08
CaO	24.30	12.64	36.52
Na <sub>2</sub> O	0.37	0.32	–
K <sub>2</sub> O	–	0.11	–
Total	99.53	96.24	99.16
<b>Normalized mineral composition</b>			
Si	1.989	7.835	2.990
Al <sup>IV</sup>	0.011	0.165	–
Al <sup>VI</sup>	0.007	0.126	1.525
Ti	0.000	0.001	0.006
Cr	0.003	–	0.000
Fe <sup>3+</sup>	0.028	0.000	0.440
Fe <sup>2+</sup>	0.267	1.685	0.000
Mn	0.012	0.035	0.008
Mg	0.673	3.123	0.009
Ca	0.983	1.992	3.020
Na	0.027	0.091	–
K	–	0.021	–
Total	4.000	15.074	7.998
<b>Molecular percent end members</b>			
Wollastonite	50.40		
Enstatite	34.48		
Ferrosilite	15.12		
Grossular			77.60
Andradite			21.60
Pyrope			0.30
Spessartine			0.28
Uvarovite			0.00
Almandine			0.00
Schorlomite			0.21

### Rhyolitic fluidal peperite

Fluidal peperite is exposed over some tens of meters on the eastern lower side of the Nea Santa rhyolite dome along its contact with a coarse-grained bio-calcurudite limestone (FP in Fig. 5). The contact is nearby and almost parallel to the northern bank of the Xiropotamos Creek and most of the year a large part of it is covered by water. Fluidal peperite has a thickness up to 2 meters and consists of ragged, wispy, sericite-altered rhyolite clasts and stringers mingled with the coarse-grained bio-calcurudite host sediment (Fig. 6). There are gradational contacts between coherent rhyolite and host sediment. The host sediment involved in the peperite is homogeneous in texture and unstratified, whereas away from peperite it is bedded (Fig. 6A,B). It is dominated by recrystallized bio-calcurudite facies, composed of carbonate granules, pebbles and limey mud, probably deposited by debris flows in a shallow submarine environment. Fossils of coral colonies of the genus *Thecosmilia* (Milne-Edwards & Haime) have been found in this facies. They are probably derived from a nearby carbonate shelf (Asvesta & Dimitriadis 2010a).

The rhyolite clasts in fluidal peperite vary in size from millimeter to decimeter. They are green in colour with small pale spots giving a speckled appearance to them. The spots are calcite-altered feldspar phenocrysts (1–3 mm in size) whereas chert-like quartz and microsparry calcite assemblages replace quartz phenocrysts, in a strongly foliated sericite-altered groundmass. The rhyolite clasts involved in fluidal peperite are more altered than the main mass of rhyolite. Ductile deformation and cleavage development have modified the primary texture and shape of the rhyolite clasts.

Crystal compositions were analysed on a Cambridge Microscan 5 electron microprobe (EMP) at the Geological Institute, in the Department of Geology and Geophysics of the University of Edinburgh, using a 20 kV accelerating potential, 30 nA incident current. Pure metals, oxides and silica combinations were used as standards. \*FeO=total Fe. Fe<sup>3+</sup> is determined based on stoichiometry and charge balance. Mineral formula calculated on a 6 Oxygen basis for pyroxene, a 23 Oxygen basis for amphibole and a 12 Oxygen basis for garnet.

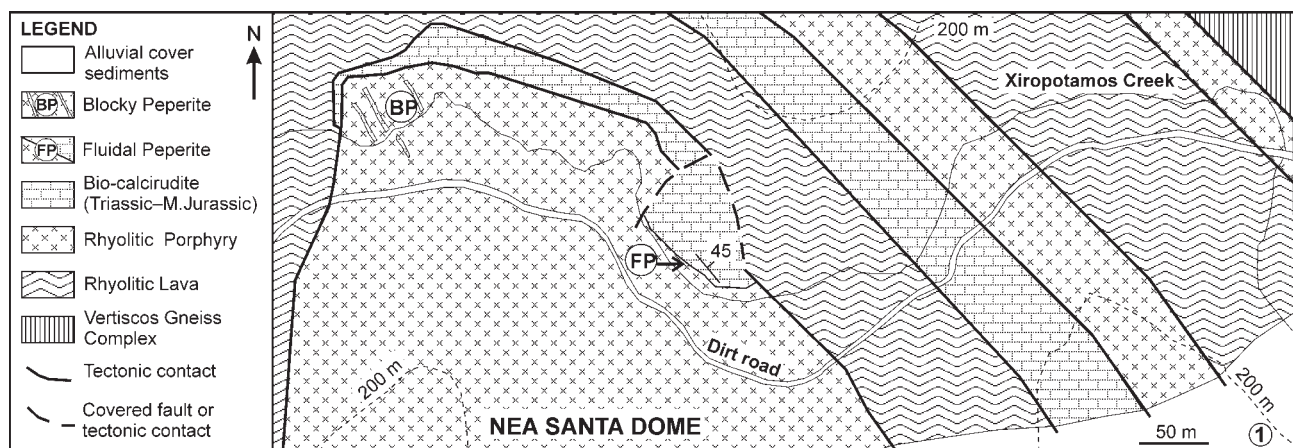


**Fig. 5.** Detailed map of the location 1 at Figure 1 showing rhyolite and carbonate sedimentary facies along the Xiropotamos Creek near Nea Santa village. Fluidal peperite (FB) is exposed on the eastern lower side of the dome and blocky peperite (BP) occurs in the western part of the dome.

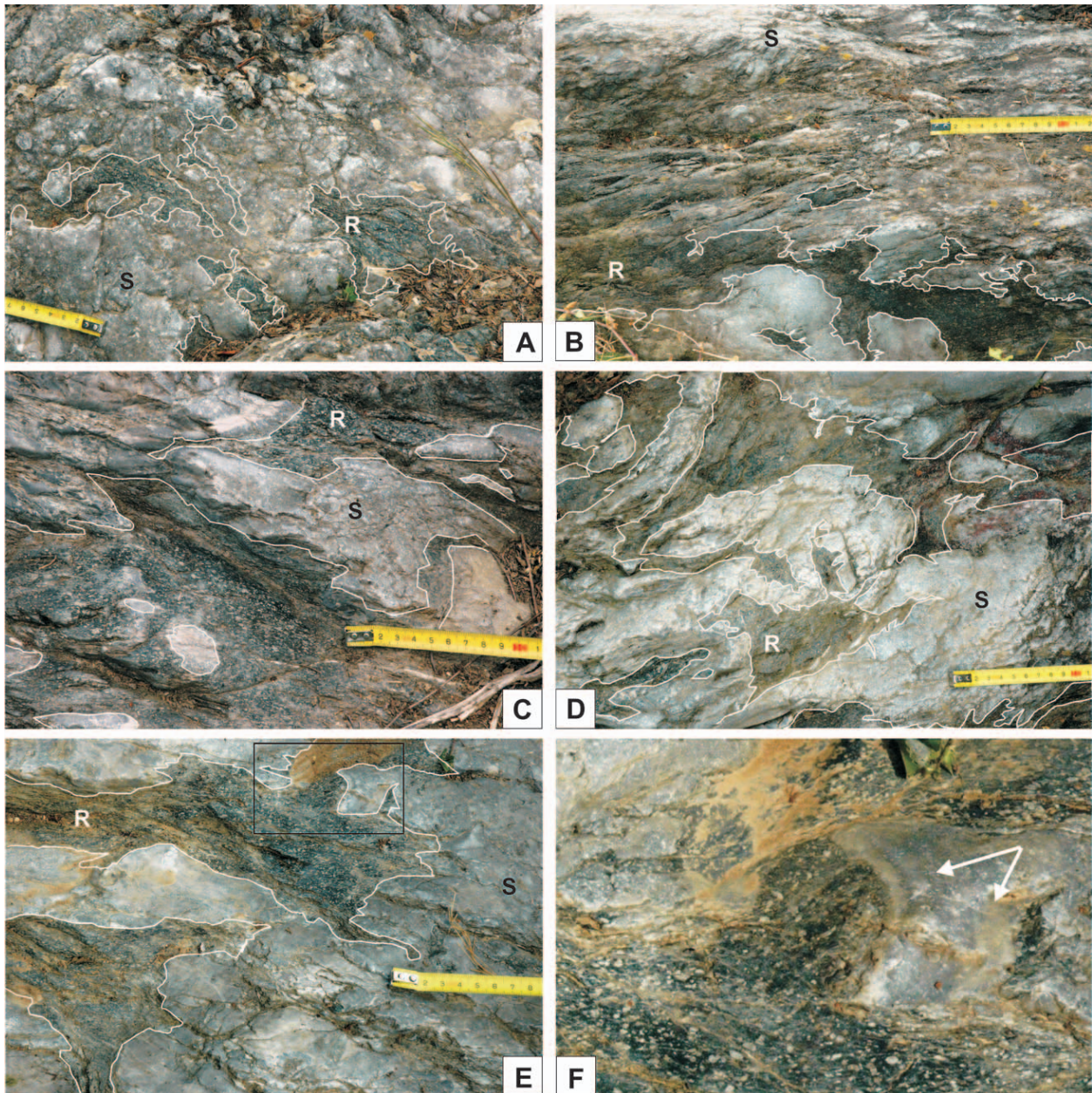


**Fig. 6.** Outcrops of fluidal peperite on the eastern lower side of the Nea Santa rhyolite dome exposed in the Xiropotamos Creek (FP in Fig. 5) showing details of the mingled domains: sericite-altered rhyolite clasts (R) and bio-calcirudite host sediment (S). Where it is possible, contacts between them are outlined. The small pale spots in the rhyolite domains are phenocrysts. **A** — Unstratified texture of the host sediment in peperite. **B** — Tongue of rhyolite (outlined) and detached clasts (two of them outlined) from the main mass of rhyolite (bottom left) within bio-calcirudite host sediment (top right). Bedding of the sediment away from rhyolite is horizontal. Cleavage is dipping  $45^\circ$  to the northeast. The outcrop is viewed to the east-northeast. **C** — Outcrop showing three-dimension relations between rhyolite and bio-calcirudite domains. Note a carbonate pebble is enclosed in the rhyolite (bottom left). **D** — Fluidal rhyolite clasts detached from the main mass of rhyolite set in bio-calcirudite host sediment. **E** — Irregular and aligned shape of the rhyolite domains is not entirely primary but a consequence of compaction and deformation. **F** — Closer view of Fig. 6E — Note bleached bands (arrows) in the host sediment that mirror the contact parallel to rhyolite clast/sediment matrix interface as a result of baking.

In some places, the carbonate sediment in direct contact with the fluidal rhyolite clasts displays macroscopic bleaching in bands parallel to the rhyolite clast/sediment matrix interface that mirror the contact (Fig. 6F). Microscopically, neofomed minerals such as microgranular chert-like silica, albite, biotite and/or chlorite are visible on the rhyolite clast/

sediment matrix interface (Fig. 7). This mineral association is confined specifically at the contact. The high concentration of quartz at the contact even though it is recrystallized and deformed probably represent an original silicification of the carbonate sediment. Bleaching and silicification of the host sediment at the contact with the rhyolite clasts are inter-

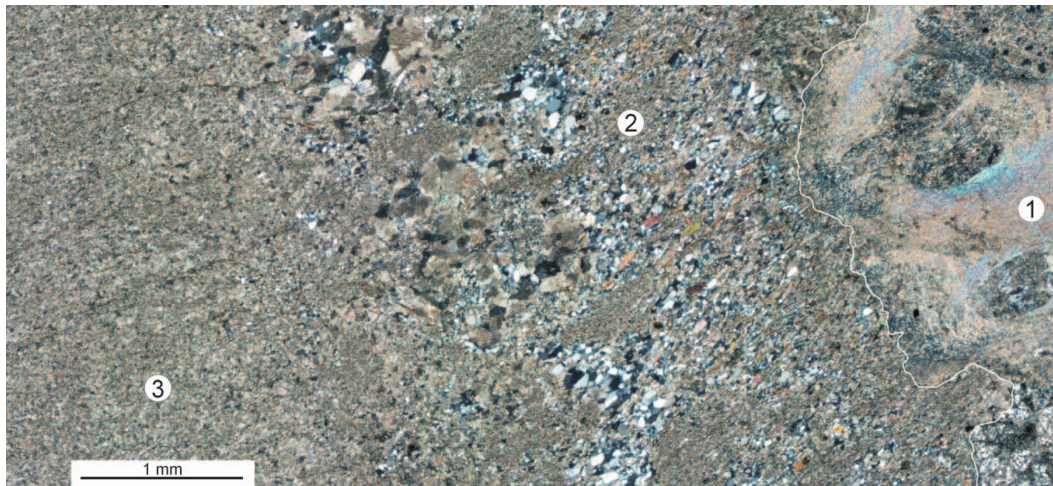


**Fig. 7.** Reaction rim in the carbonate domain indicated by the presence of neoformed minerals (quartz, albite and biotite) at the rhyolite clast/sediment matrix interface of the fluidal peperite (crossed polars). **1** — Rhyolite clast, **2** — Reaction rim, **3** — Carbonate host sediment. Interface is outlined.

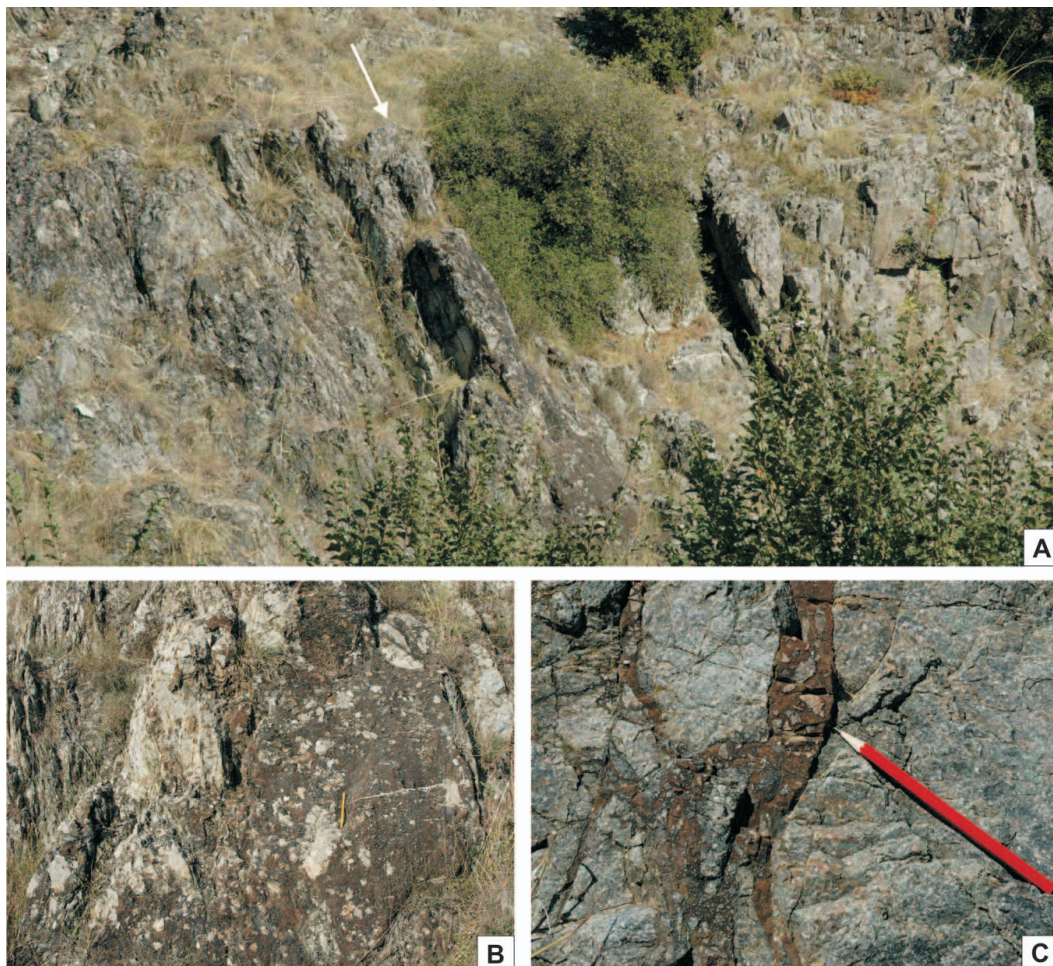


**Fig. 8. A** — Outcrop of the western part of the Nea Santa rhyolite dome at the Xiropotamos Creek (BP in Fig. 5) showing well developed prismatic columnar joints and enclosing breccia zones, viewed to the north. Note a big dyke-like breccia zone (arrow) interpreted as blocky peperite filling cooling contraction fracture. **B** — Closer view of lower middle part of previous figure. Blocky peperite occurs as a dyke-like breccia zone. The porphyry clasts (light-coloured) are blocky, polyhedral and float in the carbonate sediment matrix (brown). **C** — Blocky peperite fills cooling contraction fracture. Angular blocky jigsaw-fitted rhyolite fragments (light-coloured) reveal in situ fragmentation. The interstices are completely filled with carbonate sediment matrix (brown).

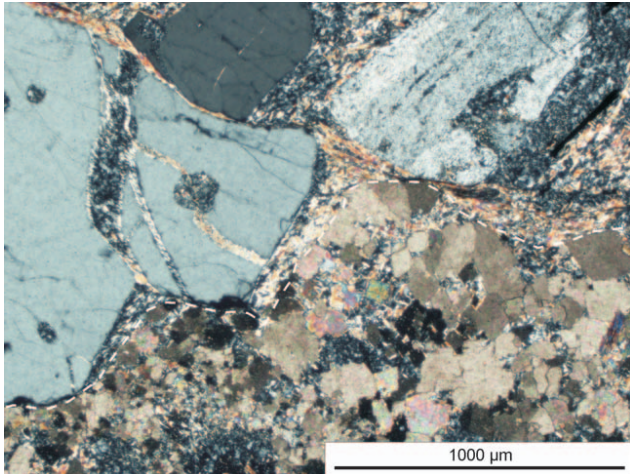


**Fig. 9.** Rhyolite clast/carbonate sediment matrix interface in the blocky porphyritic peperite (crossed polars). Rhyolite clast is composed of quartz and K-feldspar phenocrysts setting in a recrystallized groundmass (top left) and sediment matrix is composed of sparry calcite (bottom right). Boundary is outlined.

preted to reflect baking and compositional modification of the host sediment, as a result of heat and magmatic fluids rich in SiO<sub>2</sub> released from the rhyolite (cf. Hunns & McPhie 1999; Gifkins et al. 2002). It is a reaction rim at the rhyolite clast/sediment matrix contact and is formed by interaction of the hot magma and wet sediment during the formation of peperite.

*Rhyolitic blocky peperite*

Blocky peperite occurs as dyke-like breccia zones traversing the western part of the rhyolite dome (BP in Fig. 5) and fills cooling contraction fractures in prismatic columnar jointing (Fig. 8A). It consists of quartz-feldspar porphyry clasts supported in a massive recrystallized carbonate sediment matrix (Fig. 8B,C). Some fractures in the rhyolite are completely filled with sediment only. The porphyry clasts (spalls) are up to 40 cm long and many of them are blocky, polyhedral and angular with sharp corners; others however, have partly rounded margins. In places, these clasts form a jigsaw-fit texture, where clasts are not displaced far from their adjacent clasts and it is possible to

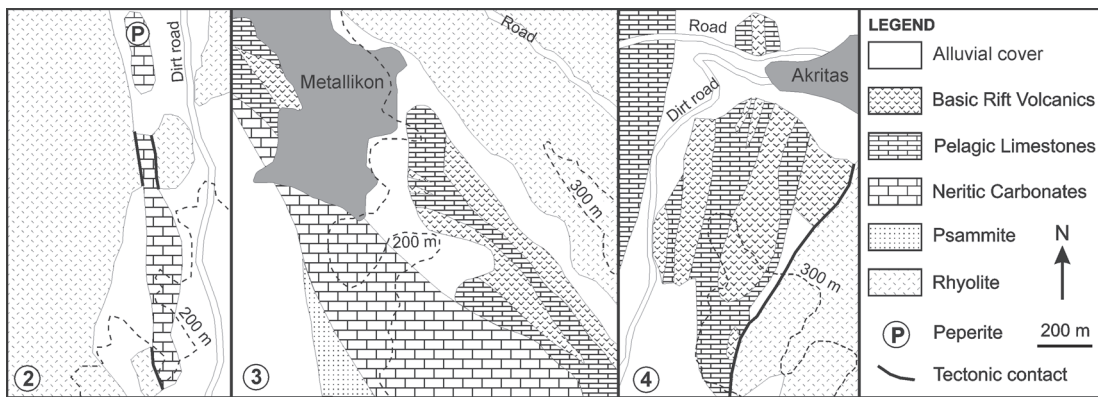


**Fig. 10.** Detailed maps 2, 3, 4 of the equivalent locations at Fig. 1.

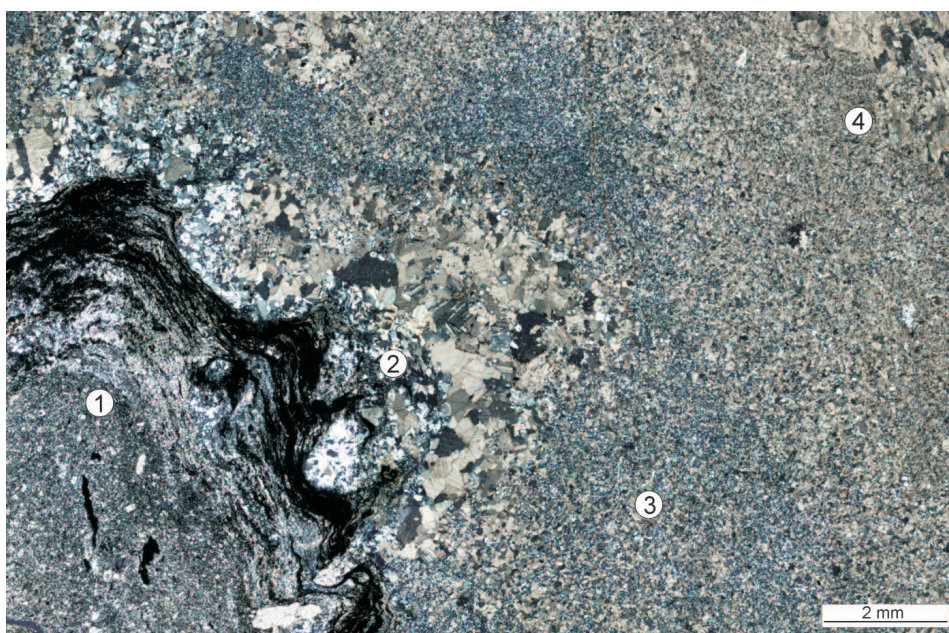


**Fig. 11.** A reaction rim at the rhyolite clast/carbonate sediment matrix interface of the Akritas peperite (crossed polars). Note the fluidal rim morphology of a rhyolite clast. 1 — Rhyolite clast, 2 — Neoformed minerals (quartz, albite and chlorite), 3 — Silicification of carbonate sediment (baked margin), 4 — Carbonate sediment.

fit clast shapes back together (Fig. 8B,C). The groundmass of the blocky porphyry clasts has been pervasively altered and metamorphosed to chert-like silica and sericite. Sparry calcite crystals also occur in the recrystallized groundmass. The phenocrysts are mostly quartz with undulose extinction and corrosion embayments filled with the recrystallized groundmass. Perthitic K-feldspar (ex-sanidine) and a small amount of sericitized plagioclase phenocrysts also occur (Fig. 9).

The carbonate sediment matrix is composed of coarse-grained sparry calcite formed by recrystallization of micrite and is locally silicified (fine-grained quartz) and dolomitized probably due to hydrothermal alteration. The extensive recrystallization, dolomitization and silicification have obscured the original sedimentary textures. Angular corroded quartz grains, kaolinitized K-feldspar and partly sericitized plagioclase from the porphyry are also dispersed in the carbonate matrix.

#### *Peperitic textures associated with the Akritas rhyolite*

To the south of Akritas village, west of Mavros Vrachos Hill (Loc. 2 in Fig. 1), tectonic slivers of Triassic limestone belonging to the Svoula Formation are emplaced in between the rhyolitic rocks of the SVS succession (map 2 in Fig. 10). A detailed macroscopic observation reveals rhyolite clasts incorporated into the limestones. Original contacts between the rhyolite and limestone have not been found.

The enclosed rhyolite clasts are porphyritic with a purple-coloured groundmass, just like the nearby rhyolite. They locally present fluidal rim morphology (Fig. 11) suggesting that they are not reworked or tectonic but juvenile. Phenocrysts are mostly quartz, K-feldspar, plagioclase and minor zircon and oxidized biotite. The groundmass has been recrystallized to quartz and sericite. The core and the rim of the clast have distinct recrystallized textures; original chilled margins cannot be recognized with certainty. Iron oxide strings also define margin parallel bands.

At its contact with the rhyolite clasts, the carbonate rock exhibits mostly microgranular chert-like quartz and little microsparry calcite. The amount of quartz diminishes away from the contact whereas sparry calcite increases (Fig. 11). This probably represents silicification of carbonate host sediment at the contact and interpreted as a baked margin (reaction rim). Neofomed minerals such as microgranular chert-like silica, albite and chlorite preferentially occur at the rhyolite clast/sediment matrix interface (Fig. 11), as in the case of the neofomed mineral assemblages of the Nea Santa fluidal peperites.

The host sediment is composed of microsparry calcite containing crinoid bioclasts. Spongy piemontite poikiloblasts with lacey borders have locally grown and contain inclusions of recrystallized calcite (Fig. 12). There are also porphyroblasts of piemontite, biotite and opaque minerals (magnetite and hematite). The sediment was apparently rich in Mn and Fe.

#### *Thermal contact phenomena in pelagic sedimentary rocks associated with the Triassic Rift Basic Volcanics*

To the south of Metallikon village (Loc. 3 in Fig. 1, map 3 in Fig. 10), zoisite crystals in a matrix of sparry calcite have

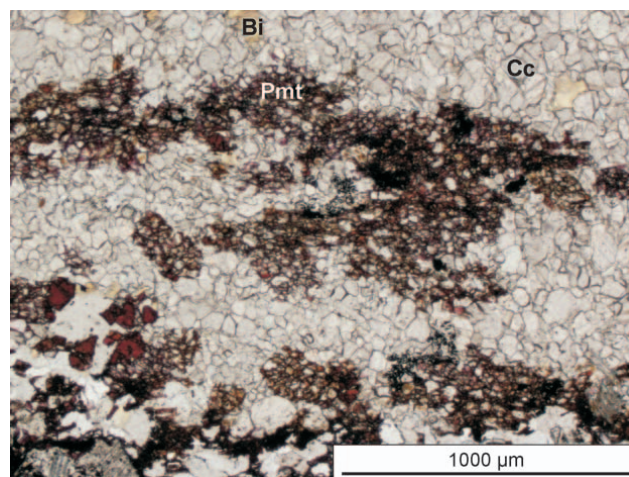


**Fig. 12.** Spongy piemontite poikiloblasts (Pmt) with lacey borders enclose sparry calcite (Cc) crystals (parallel polars). Note also biotite (Bi) crystals.

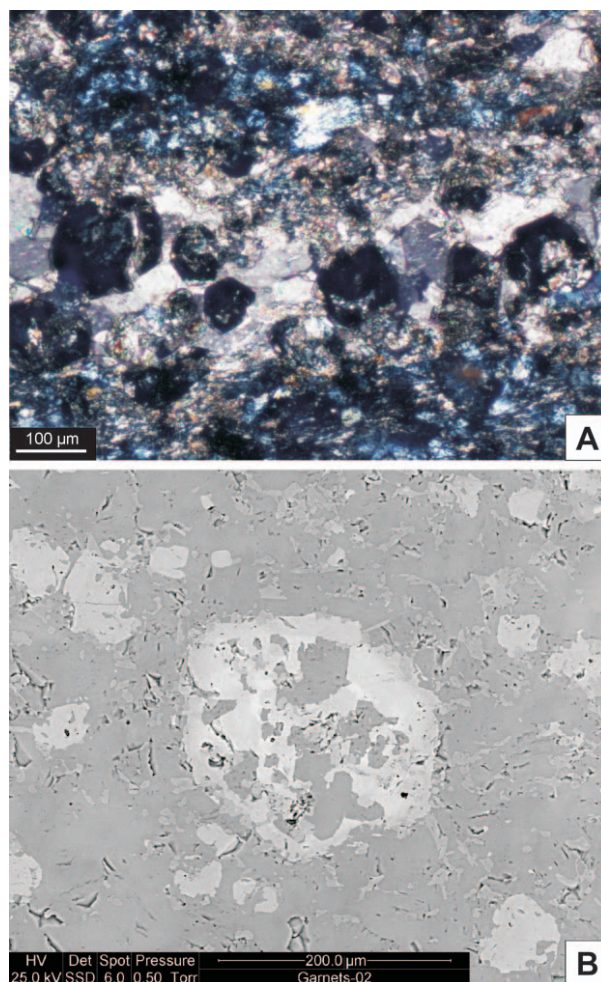


**Fig. 13.** **A** — Parallel bands composed of zoisite (anomalous blue) and garnet (isotropic) porphyroblasts and poikiloblasts in lime-marl-layered pelagic sedimentary rock that came in contact with a mafic lava; Akritas area (crossed polars). **B** — Garnet poikiloblast enclosing calcite from the carbonate matrix (SEM photomicrograph).

been developed exclusively along the margins of micritic pelagic sedimentary rocks that are in contact with mafic volcanic rocks. Their presence is taken as likely evidence of a thermal contact effect. However, more convincing evidence is found to the south of Akritas village (Loc. 4 in Fig. 1, map 4 in Fig. 10), where in the marly and limey alternating bands (1 to 10 cm thick) of the pelagic sedimentary rock that are in contact with a ~10 m thick mafic volcanic unit, abundant zoisite and tiny garnet porphyroblasts have grown in equilibrium with calcite (Fig. 13A). These two minerals are arranged in bands following the sedimentary banding. Zoisite has grown mostly in the marly bands, whereas tiny garnets (10 to 200  $\mu\text{m}$ ) are abundant in the limey bands, although they have also been nucleated at the marly bands together with zoisite. The tiny garnets (Table 2) are rich in grossular and andradite ( $\text{Gro}_{77,6}\text{Andr}_{21,6}$ ). Some of them are poikiloblasts enclosing calcite identical to that in the carbonate matrix (Fig. 13B). It is important that in this case, grossular and zoisite have grown in the marly and limey pelagic metasediment that are in contact only with the upper margin of the mafic volcanic unit, interpreted as its original base because the sequence is overturned, whereas these minerals are apparently absent from the margin of the same metasediment that is in contact with the lower margin (original top) of the mafic unit. This is convincing evidence of a thermal contact effect. It also suggests that the mafic volcanic unit in Akritas is ex-basaltic lava rather than intrusion. It furthermore weakens the possibility that the described mineral association (calcite + zoisite + garnet) is due to a metasomatic reaction related to greenschist metamorphism post-dating the basic magmatism, since in this case the reaction rims of the metasediments ought to be equally present at both their contacts with the mafic unit (with the inferred top and bottom margins of this unit).

Challis (1992) has described metamorphism of impure calcareous sediments at their contacts with a basaltic dyke at Potikirua Point, Raukumara Peninsula, New Zealand. Contact metamorphism has produced flint-hard, garnet-rich rocks. Tiny spherules of garnet of hydrogrossular and grossular-andradite (grandite) composition have been developed in thin margin parallel bands. No zoisite was formed in this case however.

## Discussion

When magma interacts with wet unconsolidated sediment, the produced features vary in character and magnitude depending on numerous factors such as: the nature of the intruded sediment, the state of its consolidation, the amount of water it contains, the viscosity of the magma, the magma volatile content and temperature, and the depth and hence the confining (lithostatic and hydrostatic) pressure of intrusion (Skilling et al. 2002 and references therein).

The positive identification of peperite requires evidence that the host sediment was unconsolidated, usually wet, at the time of mingling and that the igneous component was molten (White et al. 2000; Skilling et al. 2002). Breccia facies which are texturally similar to peperite but result from different processes may be difficult to distinguish, especially in the case of

blocky peperite. In ancient rocks, it may be difficult to distinguish blocky/angular clasts generated by tectonic processes or by fracture-controlled alteration from those generated during blocky peperite formation (Allen 1992; McPhie et al. 1993; Skilling et al. 2002). Other processes such as fallout of juvenile pyroclasts into unconsolidated sediment, water-settling of juvenile pyroclasts contemporaneous with deposition of other sediments, re-sedimentation of volcanoclastic deposits by mass flows, and infiltration of sediment into volcanoclastic deposits can all produce mixtures of igneous clasts and sediment matrix that resemble peperite (cf. Branney & Suthren 1988; White et al. 2000; Gifkins et al. 2002).

The breccia facies studied here are composed of volcanic clasts in a sediment matrix. The rhyolite clasts are interpreted as juvenile and the carbonate host sediment as wet and unconsolidated at the time of mingling. The breccias therefore are characterized as peperites. The major characteristics of the studied peperites that are assumed to be key criteria (cf. Goto & McPhie 1998; Hunns & McPhie 1999; Gifkins et al. 2002; Skilling et al. 2002; Squire & McPhie 2002; Agnew et al. 2004) for their interpretation with the sense that hot magma interacted with wet unconsolidated sediment are the following.

- The bio-calcirudite sedimentary rock in the Nea Santa fludal peperite is unstratified whereas it grades into bedded sediment away from the rhyolite. Local destruction of bedding requires that the host sediment was unconsolidated or weakly consolidated, allowing easy disruption of grain contacts.

- There are gradational contacts between coherent rhyolite and host bio-calcirudite sedimentary rock in the Nea Santa fludal peperite.

- The host carbonate sediment is bleached in a zone about 1–2 cm wide adjacent to the rhyolite clasts. The paler sediment at the contacts is more silicified than the host sedimentary facies elsewhere. Localized silicification is represented by chert-like quartz grain aggregate along the rhyolite/sediment interface. The subtle, gradational colour change and local silicification of the sediment are interpreted as results of thermal modification of the sediment (baking) in contact with hot rhyolite (McPhie 1993; Hunns & McPhie 1999; Gifkins et al. 2002).

- The highly irregular contacts between fludal rhyolite clasts and host carbonate sediment (complex clast–matrix relationships) at the Nea Santa fludal peperite suggest magma in a ductile stage.

- Fludal peperite is thought to form in cases where a water vapour film is established and maintained at the interface of the magma with the sediment. The vapour film insulates the magma from direct contact with the wet sediment, so both quench fragmentation of the magma and steam explosions are suppressed (Kokelaar 1982). According to Erkül et al. (2006), the presence of chalcidonic rims around juvenile clasts in peperite defines preserved open spaces after removal of the vapour film. Open spaces as zones of weakness at the magma/sediment interface were probably filled by hydrothermal solutions. Field evidence for vapour film development during fludal emplacement of magma at Nea Santa and Akritas peperites is found in the presence of neoformed minerals, such as: microgranular chert-like quartz, albite and biotite or chlorite, at the rhyolite clast/sediment matrix interface. Chert-like

quartz is probably the recrystallized product of original chalcidonic rims.

- The blocky angular polyhedral shape of porphyritic rhyolite clasts that commonly display jigsaw-fit texture suggests in situ fragmentation and is diagnostic of non-explosive hydroclastic mechanisms resulting from cooling and solidification of viscous magma with brittle disintegration along contraction joints.

- The presence of host sediment along cooling contraction fractures of the rhyolite suggests fluidization of sediment, in the sense of particle support and transport by a fluid, implying that the sediment was unconsolidated and probably wet at the time of peperite formation (cf. Kokelaar 1982).

The newly recognized peperite occurrences exposed near Nea Santa and Akritas villages are deformed and metamorphosed rocks, so they are not well suited to exploring some of the unanswered questions surrounding the formation of peperite. However, their recognition reveals contemporaneous magmatism and sedimentation and contributes to facies architecture and paleoenvironmental reconstruction. Silicic volcanism and accompanying neritic carbonate sedimentation during the first stages of opening of the Vardar (Axios) Basin in the Early Triassic provided locally appropriate conditions to form peperite. When the sedimentation commenced in the basin, the volcanic activities were waning but had not completely ceased. Intrusion of porphyritic rhyolitic magma during the last stage of silicic volcanism took place even contemporaneous to sedimentation and interaction between the two resulted in the formation of peperites. Due to the temporal relationship between neritic carbonate sedimentation and silicic volcanism in the Nea Santa and Akritas area, the age of the volcanic rocks can also provide constraint on the time of commencement of sedimentation in the basin.

As the rift basin evolved, mafic and minor intermediate volcanism accompanied pelagic sedimentation without forming peperitic textures. Formation of peperite may have failed due to a consolidated nature of the sediment as mafic magma was emplaced late during the evolution of the basin, when pore water in the sedimentary pile had been lost by compaction. However, the interaction of mafic magma with pelagic consolidated sediments formed contact metamorphic phenomena. The common mineral assemblage of lime-marl-layered sedimentary rocks at their contacts with the mafic rocks is: calcite + zoisite + grossular, as a result of contact metamorphism. If the growth of zoisite and grossular is also a result of metasomatism, it is difficult to write possible reactions of their formation in an open system. Moreover, regional metamorphism probably overprinted the contact metamorphism mineral assemblage and it is difficult to infer temperature and pressure conditions.

### Conclusions

In less deformed sections of the low-grade metamorphosed Silicic Volcano-Sedimentary (SVS) succession in the Circum-Rhodope Belt of northern Greece, near the Nea Santa and Akritas villages, the identification of peperitic textures at the contact margins of porphyritic rhyolite intrusions in Middle

Triassic neritic carbonate sedimentary rocks reveals evidence of interaction of silicic magma with wet unconsolidated carbonate sediments. The recognition of rhyolitic peperite is important for interpreting the facies architecture and stratigraphic relationships in the Silicic Volcano-Sedimentary (SVS) succession and timing the Triassic age of the rhyolitic intrusions.

The identification of altered basalt and dolerite intercalated with pelagic lime-marl-layered sedimentary rocks of the Metallikon and Megali Sterna Units produced the first argument for the existence of syn-sedimentary submarine mafic volcanism during the Triassic in the Circum-Rhodope Belt. Mafic volcanic rocks lack peperitic textures at their contacts with Triassic pelagic sedimentary rocks. The generation of peperite in this case was probably prevented by the consolidated nature of the sediments. However, contact metamorphic phenomena, indicated by the presence of grossular and zoisite in the margins of sedimentary rocks, are evidence of primary magmatic contacts.

**Acknowledgments:** Professor Jocelyn McPhie and one anonymous reviewer are gratefully acknowledged for suggesting significant improvements to the manuscript.

### References

- Agnew M.W., Bull S.W. & Large R.R. 2004: Facies architecture of the Lewis Ponds carbonate and volcanic-hosted massive sulfide deposits, central western New South Wales. *Aust. J. Earth Sci.* 51, 349–368.
- Allen R.L. 1992: Reconstruction of the tectonic, volcanic and sedimentary setting of strongly deformed Zn-Cu massive sulphide deposits at Benambra, Victoria. *Econ. Geol.* 87, 825–854.
- Asvesta A. 1992: Magmatism and associated sedimentation during the first stage of the opening of the Vardar oceanic basin in Triassic times. *Ph.D. Thesis, University of Thessaloniki, Greece*, 1–439 (in Greek with English summary).
- Asvesta A. & Dimitriadis S. 2010a: Facies architecture of a Triassic rift-related Silicic Volcano-Sedimentary succession in the Tethyan realm, Peonias subzone, Vardar (Axios) Zone, northern Greece. *J. Volcanol. Geotherm. Res.* 193, 245–269.
- Asvesta A. & Dimitriadis S. 2010b: The Nea Santa submarine rhyolite dome of the Triassic Silicic Volcano-Sedimentary succession, Circum-Rhodope Belt, northern Greece. *Carpathian-Balkan Geol. Assoc., XIX Congress, 23–26 September, 2010, Thessaloniki (Greece)*. In: *Geologica Balcanica, Abstracts* vol. 39, 1–2, 30–31.
- Branney M. & Suthren R. 1988: High-level peperitic sills in the English Lake District: distinction from block lavas, and implications for Borrowdale Volcanic Group stratigraphy. *Geol. J.* 23, 171–187.
- Busby-Spera C.J. & White J.D.L. 1987: Variation in peperite textures associated with differing host-sediment properties. *Bull. Volcanol.* 49, 765–775.
- Challis G.A. 1992: Hydrogarnet in contact metamorphosed calcareous sediments, Potikirua Point, Raukumara Peninsula. *N.Z. J. Geol. Geophys.* 35, 41–45.
- Dimitriadis S. & Asvesta A. 1993: Sedimentation and magmatism related to the Triassic rifting and later events in the Vardar-Axios zone. *Bull. Geol. Soc. Greece*, XXVIII(2), 149–168.
- Erkül F., Helvacı C. & Sözbilir H. 2006: Olivine basalt and trachyandesite peperites formed at the subsurface/surface interface of a semi-arid lake: An example from the Early Miocene

- Bigadiç basin, western Turkey. *J. Volcanol. Geotherm. Res.* 149, 240–262.
- Ferrière J. & Stais A. 1995: Nouvelle interprétation de la suture téthysienne vardarienne d'après l'analyse des séries de Péonias (Vardar oriental, Hellénides internes). *Bull. Soc. Géol. France* 166, 4, 327–339.
- Gifkins C.C., McPhie J. & Allen R.L. 2002: Pumiceous rhyolitic peperite in ancient submarine volcanic successions. *J. Volcanol. Geotherm. Res.* 114, 181–203.
- Goto Y. & McPhie J. 1998: Endogenous growth of a Miocene submarine dacite cryptodome, Rebun Island, Hokkaido, Japan. *J. Volcanol. Geotherm. Res.* 84, 273–286.
- Himmercus F., Reischmann T. & Kostopoulos D. 2009: Serbo-Macedonian revisited: A Silurian basement terrane from northern Gondwana in the Internal Hellenides, Greece. *Tectonophysics* 473, 20–35.
- Hunns S.R. & McPhie J. 1999: Pumiceous peperite in a submarine volcanic succession at Mount Chalmers, Queensland, Australia. *J. Volcanol. Geotherm. Res.* 88, 239–254.
- Kauffmann G. 1976: Perm und Trias im östlichen Mittelgriechenland und auf einigen ägäischen Inseln. *Z. Dtsch. Geol. Gesell.* 127, 387–398.
- Kauffmann G., Kockel F. & Mollat H. 1976: Notes on the stratigraphic and paleogeographic position of the Svoula Formation in the Innermost Zone of the Hellenides (Northern Greece). *Bull. Soc. Géol. France* (7) XVIII, 225–230.
- Kockel F. & Ioannides K. 1979: Kilkis sheet, 1:50,000 Geological Map of Greece. *Publ. I.G.M.E.*, Athens.
- Kockel F., Mollat H. & Walther H.W. 1971: Geologie des Serbo-Mazedonischen Massivs und seines Mesozoischen rahmens (Nord Griechenland). *Geol. Jb.* 89, 529–551.
- Kockel F., Mollat H. & Walther H.W. 1977: Erläuterungen zur Geologischen Karte der Chalkidhiki und angrenzender Gebiete 1:100,000, (Nord-Griechenland). *Bundesanstalt für Geowissenschaften und Rohstoffe*, Hannover, 1–119.
- Kokelaar B.P. 1982: Fluidization of wet sediments during the emplacement and cooling of various igneous bodies. *J. Geol. Soc. London* 139, 21–33.
- Kostopoulos D., Reischmann T. & Sklavounos S. 2001: Palaeozoic and Early Mesozoic magmatism and metamorphism in the Serbo-Macedonian Massif, Central Macedonia, Northern Greece. *Integrated Tectonic Studies of the Evolution of the Tethyan Orogenic Belt in the Eastern Mediterranean Region, Symposium LS03, Strasbourg, Abstracts, EUG XI*, 318.
- Kourou A. 1991: Lithology, geochemistry, tectonics and metamorphism of a part of the western Vertiscos Group. The area northeast of Lake Koroneia. *Ph.D. Thesis, University of Thessaloniki, Greece*, 1–461 (in Greek with English summary).
- McPhie J. 1993: The Tennant Creek porphyry revisited: A synsedimentary sill with peperite margins, Early Proterozoic, Northern Territory. *Aust. J. Earth Sci.* 40, 545–558.
- McPhie J., Doyle M.G. & Allen R.L. 1993: Volcanic textures: a guide to the interpretation of textures in volcanic rocks. *Centre for Ore Deposit and Exploration Studies, University of Tasmania, Hobart*, 1–198.
- Meinhold G., Kostopoulos D., Reischmann T., Frei D. & BouDagher-Fadel M.K. 2009: Geochemistry, provenance and stratigraphic age of metasedimentary rocks from the eastern Vardar suture zone, northern Greece. *Palaeogeogr. Palaeoclimatol. Palaeoecol.* 277, 199–225.
- Mercier J. 1966/68: I — Études géologique des zones internes des Hellénides en Macédoine Centrale (Grèce). II — Contribution à l'étude du métamorphisme et de l'évolution magmatiques des zones internes des Hellénides. *Thèse Doct. Ès Sciences, Univ. Paris*, 1–792 (also in: 1975, *Ann. Géol. Pays Hellén* 20, 1–792).
- Osswald K. 1938: Geologische geschichte von Griechisch-Nordmakedonien. *Geologische landesanstalt von Griechenland. Nationale Druckerei, Athen* 3, 1–141.
- Sidiropoulos N. 1991: Lithology, geochemistry, tectonics and metamorphism of the northwestern part of the Vertiscos Group. The area of Mount Dysoro (Krousia) north of Kilkis. *Ph.D. Thesis, University of Thessaloniki, Greece*, 1–592 (in Greek with English summary).
- Skilling I.P., White J.D.L. & McPhie J. 2002: Peperite: a review of magma-sediment mingling. *J. Volcanol. Geotherm. Res.* 114, 1–17.
- Squire R.J. & McPhie J. 2002: Characteristics and origin of peperite involving coarse-grained host sediment. *J. Volcanol. Geotherm. Res.* 114, 45–61.
- Stais A. & Ferrière J. 1991: Nouvelles données sur la paleogeographie Mesozoïque du domaine Vardarien: Les bassins d'Almopias et de Peonias (Macédoine, Hellenides Internes Septentrionales). *Bull. Geol. Soc. Greece* XXV(1), 491–507.
- Tsamadouridis P. & Choriantopoulou P. 1990: Geological-metallurgical approach of the banded iron formation in volcano-sedimentary rocks of the Mavros Vrachos area of Kilkis. *Bull. Geol. Soc. Greece* XXII, 139–158 (in Greek with English abstract).
- White J.D.L., McPhie J. & Skilling I.P. 2000: Peperite: a useful genetic term. *Bull. Volcanol.* 62, 65–66.
- Winchester J.A. & Floyd P.A. 1977: Geochemical discrimination of different magma series and their differentiation products using immobile elements. *Chem. Geol.* 20, 325–343.